The LHCb Silicon Tracker*

B. Adeva[a], A. Gallas[a], E. Pérez Trigo[a], P. Rodríguez Pérez[a], Y. Amhis[b,f], A. Bay[b], F. Blanc[b], G. Cowan[b,g], F. Dupertuis[b], V. Fave[b], G. Haefeli[b], I. Komarov[b], J. Luisier[b], R. Märki[b], B. Muster[b], T. Nakada[b], O. Schneider[b], M. Tobin[b], M.T. Tran[b], J. Anderson[c], A. Bursche[c], N. Chiapolini[c], M. De Cian[c,h], Ch. Elsasser[c], C. Salzmann[c], S. Saornil[c], S. Steiner[c], O. Steinkamp[c], U. Straumann[c], A. Vollhardt[c], O. Aquines Gutierrez[d], M. Britsch[d], M. Schmelling[d], H. Voss[d], V. Iakovenko[e], O. Okhrimenko[e], V. Pugatch[e]

a University of Santiago de Compostela, Santiago de Compostela, Spain.

b Ecole Polytechnique Fédérale de Lausanne (EPFL), Lausanne, Switzerland.

c Physik-Institut, Universität Zürich, Zürich, Switzerland.

d Max Planck Institut für Kernphysik (MPIK), Heidelberg, Germany.

e National Academy of Sciences, Institute for Nuclear Research, Kiev, Ukraine.

f Now at LAL, Université Paris-Sud, CNRS/IN2P3, Orsay, France.

g Now at School of Physics and Astronomy, University of Edinburgh, Edinburgh, United Kingdom.

h Now at Physikalisches Institut, Ruprecht-Karls-Universität Heidelberg, Heidelberg, Germany.

LHCb-PROC-2013-022
06/08/2013

Abstract

The LHCb experiment is designed to perform high-precision measurements of CP violation and search for new physics using the enormous flux of beauty and charm hadrons produced at the LHC. The LHCb detector is a single-arm spectrometer with excellent tracking and particle identification capabilities. The Silicon Tracker is part of the tracking system and measures very precisely the particle trajectories coming from the interaction point in the region of high occupancies around the beam axis. The LHCb Silicon Tracker covers a total sensitive area of about 12 m^2 using silicon micro-strip detectors with long readout strips. It consists of one four-layer tracking station before the LHCb dipole magnet and three stations after. The detector has performed extremely well since the start of the LHC operation despite the fact that the experiment is collecting data at instantaneous luminosities well above the design value. This paper reports on the operation and performance of the Silicon Tracker during the Physics data taking at the LHC during the last two years.

*Submitted to Proceedings of 13th Vienna Conference on Instrumentation.

1 Introduction

The LHCb experiment [1] is dedicated to the study of heavy flavour physics in proton-proton collisions at the LHC. The primary goal of LHCb is to make indirect searches for new physics in precision measurements of CP violation and rare decays of b and c hadrons. The detector is a single arm forward spectrometer which covers the pseudorapidity range between 2 and 5 to take advantage of the fact that b-pairs are predominantly produced close to the direction of the beam at the LHC.

The LHCb Silicon Tracker (ST) consists of two silicon micro-strip detectors located before and after a 4 Tm dipole magnet. The Tracker Turicensis (TT) is 150 cm wide and 130 cm high and covers the full acceptance upstream of the magnet. The Inner Tracker (IT) is situated in a 120 cm by 40 cm cross-shaped region in the centre of three planar tracking stations downstream of the magnet. The IT covers the region around the beam pipe with the highest density of tracks corresponding to around 1.2% of the total acceptance. The total sensitive area in the TT and IT is 8 m^2 and 4.2 m^2 respectively.

The TT consists of four detection layers with strips oriented at (0°, +5°, -5°, 0°) with respect to the vertical axis. The detector uses 500 μm thick p-on-n sensors with a strip pitch of 183 μm. Sensors are bonded together to provide readout sectors with different length strips (up to 37 cm). There are 280 readout sectors and 143600 readout channels.

Each of the IT stations is constructed from four independent boxes arranged around the beam-pipe. An IT box contains four detection layers with the same orientation as those in the TT. The boxes either side of the beam pipe contain modules with 410 μm thick p-on-n sensors and a strip length of 22 cm. The modules in the boxes above and below the beam pipe are 11 cm long and 320 μm thick. The strip pitch is 198 μm in both cases. There are 336 readout sectors and a total of 129024 readout channels.

The electronic readout is essentially the same for both detectors. Analogue signals from the silicon strip detectors are amplified by the Beetle front end chip [2] and transmitted via copper cables to service boxes located outside the acceptance. The service boxes contain digitiser boards where the signal is digitised and transmitted via VCSEL diodes to the TELL1 [3] readout board in the counting house. The TELL1 board uses FPGAs to perform pedestal subtraction, common mode noise subtraction and zero suppression of the data.

2 Detector Performance

2.1 Time Alignment

The data collected during the first proton-proton collisions were used to time align the detector with respect to the LHC collisions. The time alignment procedure ensures that trigger and control signals are synchronised within LHCb and takes into account differences in cable lengths as well as the time of flight for particles passing each station. The optimal delays were determined using a scan over the delay between the sampling time of the front-end electronics and the trigger time with respect to the LHC clock. The delays were varied in steps of 6.5 ns and the most probable value (MPV) of the charge distribution was determined for each delay setting from a fit to a Landau convolved with a Gaussian. The peak of the pulse shape as a function of time was found by fitting the expected front-end signal shape to the distribution of the MPV versus the delay. The internal time alignment of the detector is known to better than 1 ns.

2.2 Signal to Noise Ratio

The signal to noise ratio (S/N) for clusters on tracks reconstructed with a momentum greater than 5 GeV was found to be in the range 12 to 15 for the TT, and 16.5 and 17.5 for the long and short ladders in the IT. The distribution of the S/N measured in the TT is shown in Fig. 1 as a function of the input capacitance of the strip. The MPV determined for each of the sectors in the IT is shown in Fig. 1. The values are in good agreement with those expected from prototype measurements.

2.3 Spatial Alignment

A global χ^2 minimisation based on Kalman track residuals [4] was used to perform the spatial alignment of the detectors. The method was extended to include vertex information from $D^0 \to K^-\pi^+$ decays and applying constraints to their invariant mass [5]. The unbiased residuals, calculated by removing a hit from the track fit and computing the distance between the hit and the extrapolated track position, are shown in Fig. 2 (left) for all IT clusters on tracks. The so-called biased residual, defined as the mean of the unbiased residual distribution for each sector, is also shown in Fig. 2 (right) for all IT sectors. The RMS of the biased residual distribution gives an estimate of the precision of the alignment procedure and was found to be around 14 μm for both TT and IT. The single hit resolution can be extracted by

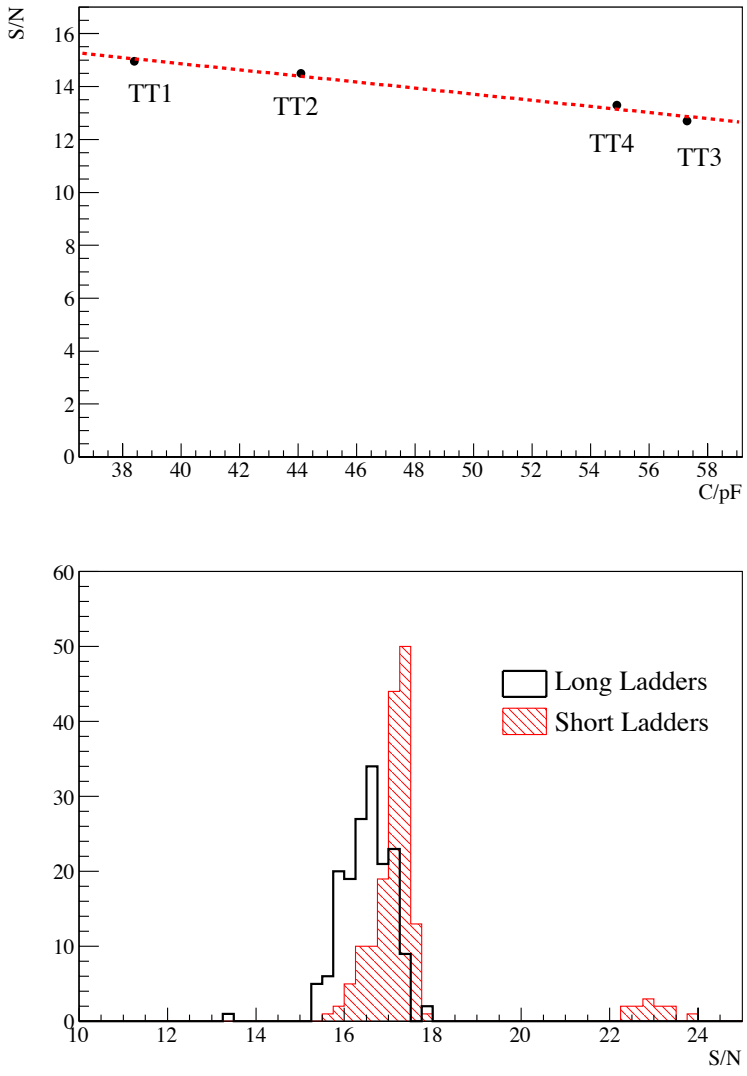

Figure 1: Measured signal to noise ratio as a function of strip capacitance in TT (top) and for the two different strip lengths in IT (bottom). A second peak around 23 in the distribution of the S/N for the short ladders is visible because some 410 μm sensors were used during the module production instead of the 320 μm sensors.

removing the contribution due to the alignment procedure from the unbiased residuals. The hit resolution was measured to be 59 μm and 50 μm for the TT and the IT respectively.

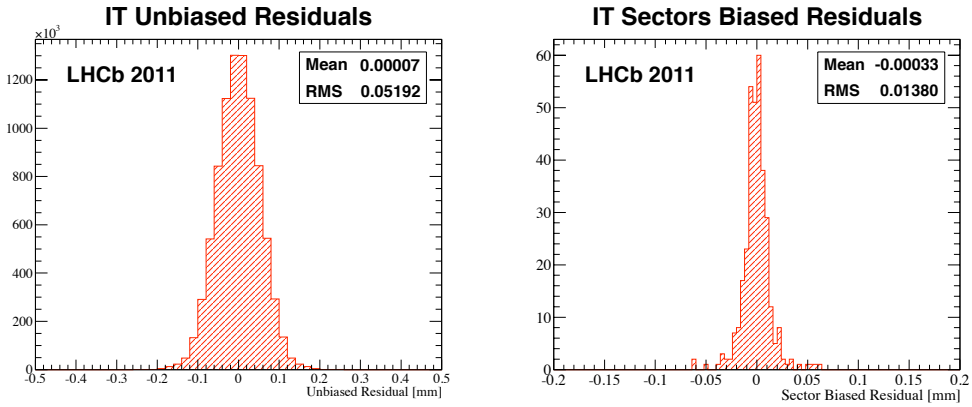

Figure 2: Distribution of the unbiased (left) and biased (right) residuals in the IT.

2.4 Hit Efficiency

The hit efficiency was measured using isolated tracks with a momentum greater than 10 GeV. The clusters in each sensor were excluded from the track fit in turn and a search was made for clusters in a window around the track. The hit efficiency is defined as the ratio of the number of hits found to the number of hits expected. The efficiency depends on the size of the window used and the maximum efficiency was measured to be 99.3% for IT and 99.7% for TT.

3 Radiation Damage

The geometry of the LHCb detector means that the flux of particles across the IT and TT is highly non-uniform. The fluence expected after ten years of nominal LHC operation[1] was 5×10^{13} and 8×10^{13} 1-MeV neutron equivalent per cm^2 for the TT and IT respectively. This means that type inversion of the silicon would occur within the first two years of operation for the sensors closest to the beam-pipe.

[1]Assuming a centre of mass energy of 14 TeV and an integrated luminosity of 2 fb^{-1} per year.

The running conditions in the first three years of operation were much different from the design. The detector took data at much higher instantaneous luminosities and pile-up by using a so-called luminosity levelling process. The vertical beam separation is reduced during a fill so that a constant luminosity can be maintained. The total integrated luminosity delivered to LHCb during the first three years of operation was around 3.4 fb^{-1}. Two different methods are used to monitor the radiation damage in the detectors and they are described in the following sections.

3.1 Leakage Current

The measured leakage current provides an excellent probe of the radiation damage as the change in current is directly proportional to the observed fluence. The current is constantly monitored and the maximum current in each fill is shown in Fig. 3 as a function of time for the IT modules. This figure also shows the integrated luminosity as a function of time and it can clearly be seen that the leakage current increases as expected with the delivered luminosity. Decreases in the measured current are also visible. These are caused by changes in the operating temperature of the sensors as well as annealing during the winter shutdowns. The nominal operation temperature is around 8°C.

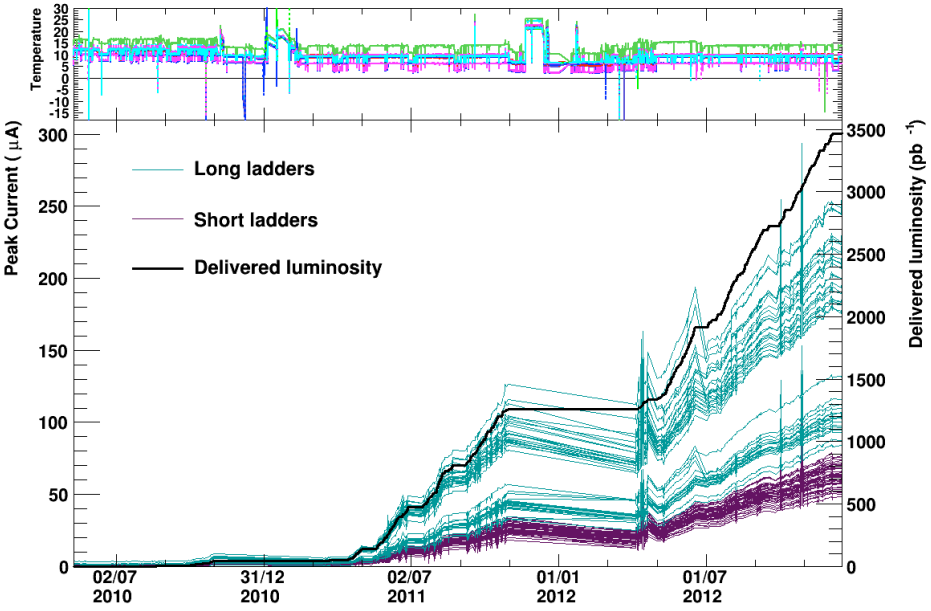

Figure 3: Measured leakage current in the IT as a function of time. The temperature of the IT boxes is also shown.

The expected change in current is $\Delta I = \alpha\phi V$ where V is the volume of the sensor, ϕ is the fluence and α is the current related damage rate which depends on the temperature and the annealing. The value of the current at a temperature T_1 can be corrected to another temperature, T_2 using the relation:

$$\frac{\mathrm{I(T_2)}}{\mathrm{I(T_1)}} = \left(\frac{\mathrm{T_2}}{\mathrm{T_1}}\right)^2 \exp\left(-\frac{\mathrm{E_g}}{2\mathrm{k_B}}\left(\frac{1}{\mathrm{T_2}} - \frac{1}{\mathrm{T_1}}\right)\right)$$

where k_B is the Boltzmann constant and a value of 1.21 eV was used for the energy gap, E_g [6, 7].

The measured current and is shown in Fig. 4 together with the expected leakage current as a function of the delivered luminosity for the TT sensors which are located around to the beam-pipe. The currents have been corrected to 0°C and show excellent agreement between the expected and measured values.

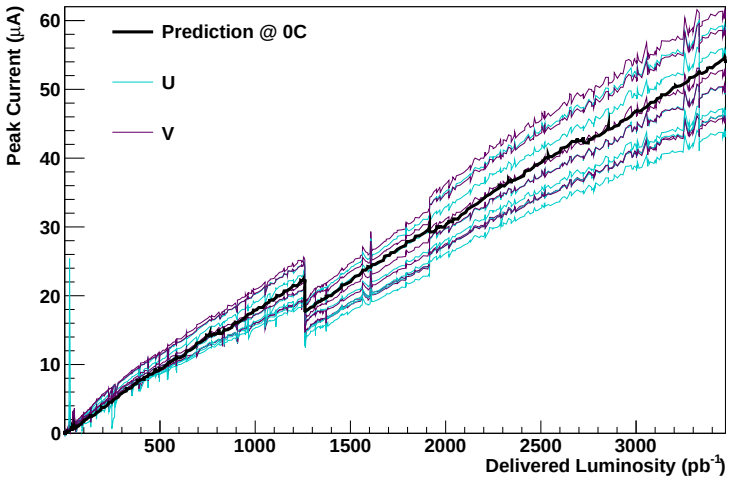

Figure 4: Leakage current as a function of the delivered luminosity for the sensors closest to the beam-pipe in the TT stereo layers (U/V $\equiv +5°/-5°$).

3.2 Depletion Voltage

The change in the depletion voltage is measured using three dedicated charge collection efficiency scans taken during the year. The maximum charge is extracted from a mini-pulseshape scan (cf. Sec. 2.1) for different values of the bias voltage. The most probable value is plotted as a function of the bias

voltage and a sigmoid function, defined as

$$ADC_{max}(V_{bias}) = \frac{A_0}{1 + \exp r(V_{bias} - V_0)},$$

is fitted to this distribution. An example is shown in Fig. 5.

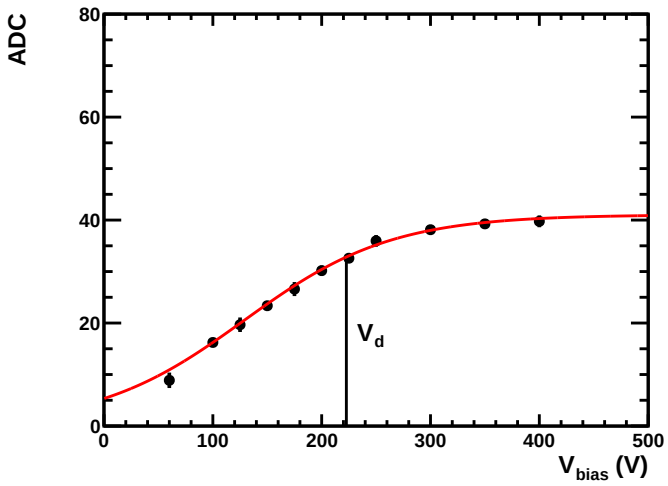

Figure 5: The charge in ADC counts as a function of the bias voltage for one scan. The extracted depletion voltage, V_d, in indicated by a line.

The depletion voltage is taken to be the point where the fitted function is 80% of its maximum value. This value was chosen such that the depletion voltage extracted from the first scan, when the detector had not been exposed to much radiation damage, matched the depletion voltage measured directly from capacitance voltage scans during the construction of the detector. The expected depletion voltage is calculated using the Hamburg model [6] and a simulation of the particle fluxes in the detector [8]. The measured and expected depletion voltage agrees as shown in Fig. 6 for an example TT sector.

4 Detector Operation

There were a few problems encountered during the construction and operation of the detector. A selection of the most interesting are described in the following sections.

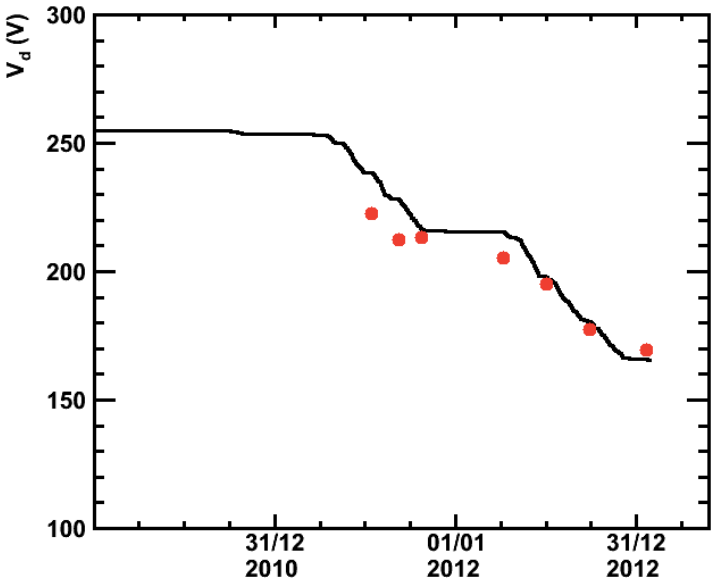

Figure 6: The depletion voltage measured during the different charge collection efficiency scans for one sector in the TT (dots). Also shown is the expected depletion voltage (line) which was calculated using the Hamburg model.

4.1 VCSEL Diodes

The fraction of working channels in the TT and the IT was 99.62% and 98.71% respectively at the time of this conference. The inefficiency in the TT is dominated by the occasional death of the VCSEL diodes used to transmit the optical data to the pre-processing boards. However, the design and location of the TT electronics allows these broken VCSELs to be replaced during short LHC Technical Stops. Access to the IT electronics requires the tracking stations to be opened. This is considered a too great risk to be performed regularly so broken VCSELs in the IT are only replaced during the long winter shutdowns. There are also two modules in IT which cannot be configured. It is planned that repairs will be made during the LHC LS1 in 2013/14.

4.2 Broken Bonds in TT

A problem was observed for some modules in the TT after they had been installed. A low RMS noise appeared on every fourth channel in a readout chip as shown in Fig. 7. This low noise was caused by broken bond wires between the innermost bond row on the chip and the pitch adaptor. The bond

height used was too low so new hybrids were constructed with an increased distance between the pitch adaptor and the chip. A total of nine modules were removed from the detector and repaired during the shutdown in 2010. No problems have been seen since they were reinstalled.

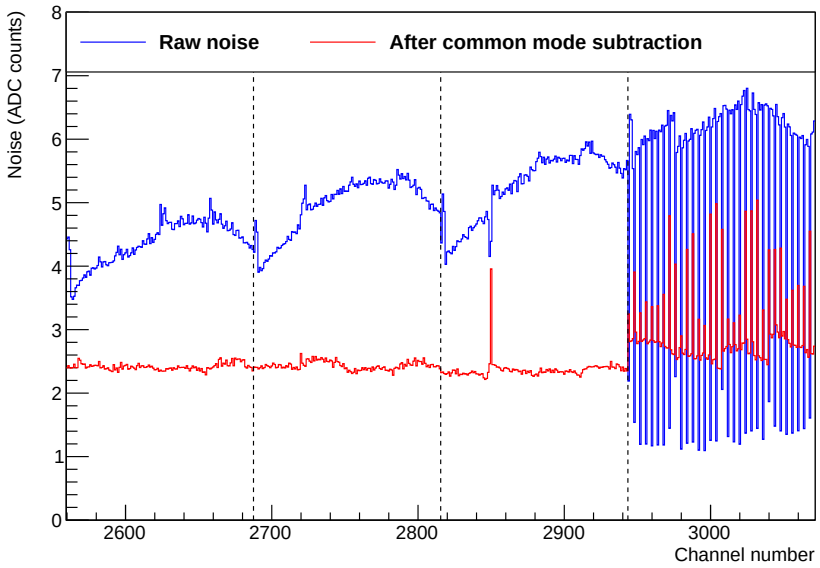

Figure 7: The noise for each channel in a sector with broken bonds between the last readout chip and the pitch adaptor. The broken bonds are observed on every fourth channel from 2944 to 3068.

4.3 High Currents in TT

Abnormally high currents were observed during the early data taking in 2010 and 2011. The leakage current was expected to be below 10 μA but currents of the order of hundreds of μA were seen. The current would rise suddenly and then decrease slowly over the course of a fill as shown in Fig. 8. In the most extreme case, this caused a number of high voltage channels to trip in the power supply leading to large dead regions in the detector. This effect was only observed for the modules in the layers closest to the walls of the detector box.

It was also observed that the spikes in the current were partially correlated with the instantaneous luminosity as shown in Fig. 9. This effect was seen in the early data taking period where the LHC was running with lower instantaneous luminosities than the nominal value. This could have limited the ability of the experiment to collect data with a high effeciency at higher

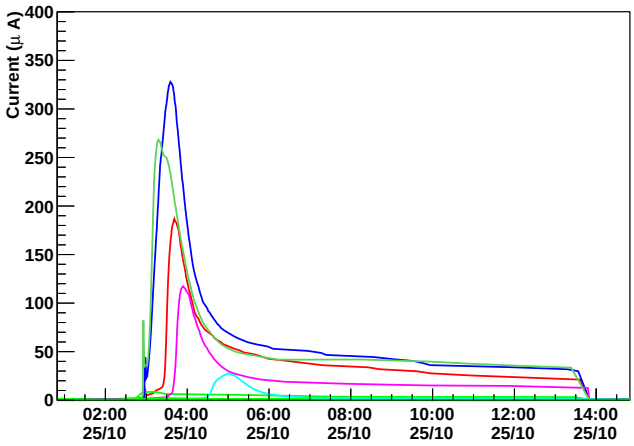

Figure 8: The measured current in a fill as a function of time.

instantaneous luminosities if the currents continued to rise and, therefore, cause the power supply to trip. The modules could have been disabled but this would have resulted in large gaps in the detector coverage. The bias voltages applied could be reduced but this would decrease the hit efficiency in the sensors if they were operated below their full depletion voltage.

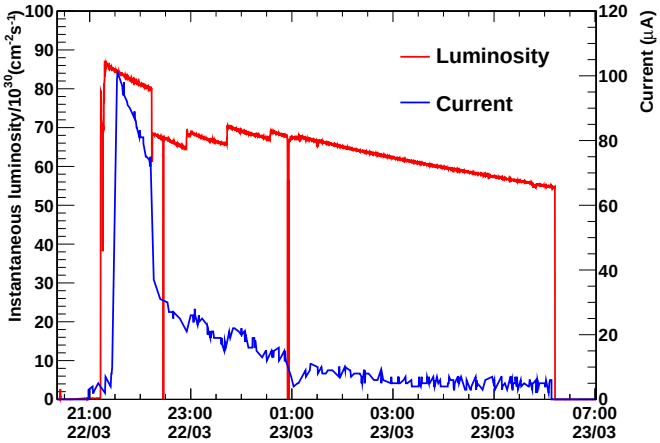

Figure 9: The current as a function of time is shown together with the instantaneous luminosity for a fill taken during the early part of 2011. The steps made in the luminosity levelling process can also be seen in the measured current.

Various different solutions were tried to solve the problem. The problematic modules were operated with slightly reduced bias voltages and trip

limits were increased to improve the data taking efficiency. The problem was cured by installing Kapton shielding on the walls of the detector box and changing the operation procedures so that the high voltage is kept on during inter-fill periods. The mechanism behind this effect is not understood.

5 Conclusions

The LHCb Silicon Tracker has performed admirably during the first three years of LHC operation. The measured radiation damage is found to be in good agreement with that expected from simulation. A number of problems were encountered during the first years of operation which have been solved.

References

[1] LHCb Collaboration, JINST 3 S08005 (2008).

[2] M. Agari *et al.*, Nucl. Inst. Meth. A518 (2004) 468.

[3] G. Haefeli *et al.*, Nucl. Inst. Meth. A560 (2006) 494.

[4] W. Hulsbergen, Nucl. Inst. Meth. A600 (2009) 471-477.

[5] J. Amoraal *et al.*, Nucl. Inst. Meth. A712 (2013) 48-55.

[6] M. Moll *et al.*, Nucl. Inst. Meth. A426 (1999) 87.

[7] A.Chilingarov, Technical Note RD50-2011-01 (2011)

[8] M. Siegler *et al.*, CERN-LHCb-2004-070 (2004).